Theoretical Determination of the Singlet → Singlet and Singlet → Triplet Electronic Spectra, Lowest Ionization Potentials, and Electron Affinity of Cyclooctatetraene

Luis-Manuel Frutos[†] **and Obis Castaño***[,‡]

Departamento de Química Física, Universidad de Alcalá, Alcalá de Henares, ES-28871 Madrid, Spain

Manuela Merchán*[,§]

Departamento de Química Física, Instituto de Ciencia Molecular, Universitat de València, Dr. Moliner 50, Burjassot ES-46100 Valencia, Spain

Received: February 11, 2003; In Final Form: May 14, 2003

The singlet → singlet and singlet → triplet electronic spectra of cycloocta-1,3,5,7-tetraene are studied using multiconfigurational second-order perturbation theory (CASPT2) and extended atomic natural orbitals (ANOs) basis sets. The observed dipole-allowed features at 4.43, 6.02, and 6.42 eV and the spin-forbidden singlet → triplet bands with maxima at 3.05, 4.05, and 4.84 eV (Frueholz, R. P.; Kuppermann, A. *J. Chem. Phys.* **1978**, *69*, 3614) are assigned as the transitions $1^1A_1 \rightarrow 1^1A_2$, $1^1A_1 \rightarrow 2^1B_2(3p_z)$, $1^1A_1 \rightarrow 3^1E$, and $1^1A_1 \rightarrow 1^3A_2$, $1^1A_1 \rightarrow 1^3E$, $1^1A_1 \rightarrow 1^3B_1$, respectively. The lowest (3s) Rydberg singlet and triplet states are placed at 5.58 (2^1A_1) and 5.54 (1^3A_1) eV. New assignments are tentatively suggested for the recorded higher-energy peaks in the singlet manifold. The three lowest ionization potentials are also characterized. At the highest level of theory, the computed adiabatic electron affinity is 0.56 eV, in agreement with experimental determinations. As regards the role of cyclooctatetraene as an efficient triplet quencher of laser dye solutions, the computation supports it could act as acceptor with donors having a triplet excited-state energy equal to or higher than 0.8 eV.

1. Introduction

Considerable effort has been devoted to understand the thermal and photochemical reactivity of cyclooctatetraene (COT hereafter) from both experimental and theoretical standpoints (for a recent review see Garavelli *et al.*[1]). The electronic spectra of COT have comparatively received less attention, and only a few experimental[2−4] and theoretical[1,5−8] studies are available. The ground state in the gas phase determined by electron diffraction (ED) techniques has a tub-shaped structure with alternating bond lengths.[9] Theoretical calculations[1,8] have also repetitively predicted a ground-state structure belonging to D_{2d} symmetry consistent with the ED data. The COT molecule has been considered along the years a classic prototype of a cyclic nonaromatic hydrocarbon. Because of its nonplanar structure, through-bond and through-space interactions between the double bonds have to be taken into account in the theoretical description of the excited states. The implied difficulties in the ab initio characterization of the electronic spectra of COT are more closely related to a strained, nonplanar diene like norbornadiene (bicyclo[2.2.1]hepta-2,5-diene)[10] than to even polyenes such as *all-trans*-1,3,5,7-octatetraene.[11] Apart from the intrinsic interest, characterization on theoretical grounds of the singlet → singlet and singlet → triplet spectra can give further insight to the understanding of the behavior of COT as a triplet quencher. The use of COT as an efficient triplet scavenger for several laser dye solutions is well-known,[12,13] and the detailed mechanism for the energy-transfer process has been recently analyzed.[14] In this context, a high-level ab initio description of the electronic spectra of COT seems to be appropriate at present. We report here a comprehensive theoretical research study of the excited states of COT, of both valence and Rydberg nature.

The gas-phase optical absorption of COT can be described as a broad band of low intensity over the region 310−260 nm (4.00−4.77 eV) with a maximum at 4.39 eV and an intense band with a shoulder at 6.05 eV and a maximum at 6.42 eV (limit of the experimental study).[5,8] These singlet → singlet transitions were also observed by electron energy-loss spectroscopy (EELS)[3] at 4.43, 6.02, and 6.42 eV. In addition, Frueholz and Kuppermann[3] identified three singlet → triplet features with an intensity maximum at 3.05, 4.05, and 4.84 eV and several singlet → singlet transitions at higher energies up to 14 eV. No clear experimental identification of the lowest Rydberg states was, however, possible, and the assignments performed by these authors were strongly biased by previous semiempirical results where only valence excited states could be calculated.[3] As discussed below, the lowest Rydberg state of COT is firmly predicted from our results around 5.6 eV, and the transition from the ground to a 3p-Rydberg state computed at 6.17 eV is proposed as the most plausible candidate for the recorded shoulder at about 6 eV.[3,5,8] The latter was previously associated with a valence feature.[3]

The excited states of COT are characterized by using multiconfigurational second-order perturbation theory through the CASPT2 method.[15,16] The successful performance of the CASPT2 approach in computing spectroscopic properties is well established.[17−19] We believe that the present results provide a more complete picture for a better understanding of the spectroscopic behavior of the system and allow us to make confident assignments. The present research includes analysis of the vertical transitions related to the singlet → singlet and singlet → triplet spectra,[3] assignments for the lowest ionization potentials (IPs)[20−22] of the COT molecule, computation of the

† E-mail: luisma.frutos@uah.es.
‡ E-mail: obisd.castano@uah.es.
§ E-mail: manuela.merchan@uv.es.
* Corresponding author.

10.1021/jp030193n CCC: $25.00
Published on Web 06/21/2003

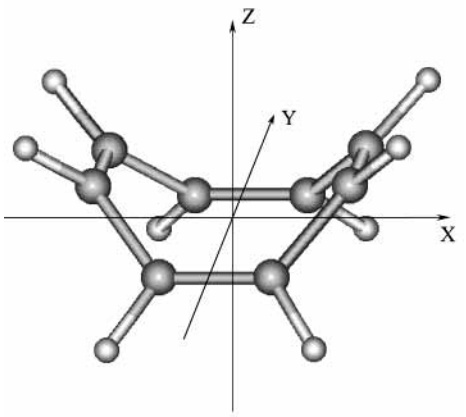

Figure 1. Orientation of the cycloocta-1,3,5,7-tetraene molecule (D_{2d} symmetry).

main features of the photoelectron (PE) spectrum of the cyclooctatetraene radical anion (COTRA),[23,24] determination of the adiabatic electron affinity (EA) for the neutral system,[25] and an estimate for the band origin of the lowest singlet → triplet transition. The latter issue is particularly relevant to support the nonvertical triplet energy transfer mechanism to COT, behaving as acceptor, in a quenching process.[12] We shall find that a number of previous assignments are clearly confirmed, but the situation is shown to be even more complex in certain cases and new interpretations are then offered. The current results serve both to complement earlier studies and to bring a firm foundation for a theoretical elucidation of some aspects involved in the rich photochemistry of COT.

The paper is organized as follows. Computational details are described in the next section. Results and analysis on the computed singlet → singlet spectrum, IPs, low-lying triplet states, EA, and PE spectrum of COTRA are subsequently considered, together with comparison to previous findings. In light of the present results, the role of COT in laser dye quenching is finally discussed. Our conclusions are summarized in the last section.

2. Theoretical Methods and Computational Details

Generally contracted basis states of atomic natural orbital (ANO)-type obtained from the C(14s9p4d)/H(8s4p) primitive sets with the C[4s3p1d]/H[2s1p] contraction scheme[26] were used for the geometry optimization of the ground state at the CASSCF level.[27] Actual calculations were performed in C_{2v} symmetry, imposing symmetry constraints of the D_{2d} symmetry both in the variation of the geometric parameters and in the CASSCF wave function. The orientation of the molecule is depicted in Figure 1.

The closed-shell restricted Hartree−Fock wave function has 28 occupied molecular orbitals (MOs) denoted by (5;7;4;3;2), where the entries indicate the number of occupied MOs belonging to the irreducible representations a_1, e, b_2, b_1, and a_2 of the D_{2d} point group. In the present case, with the mapping D_{2d}/C_{2v} $a_1 + b_2/a_1$, $e/b_1 + b_2$, $b_1 + a_2/a_2$, the SCF wave function can be represented by (9;7;7;5), corresponding to the number of occupied MOs of the a_1, b_1, b_2, and a_2 symmetries of the C_{2v} point group. For the ground-state geometry optimization, the π-valence space was employed. It comprises eight active electrons distributed among the eight π valence MOs, (2;2;2;2) in C_{2v} symmetry, keeping the remaining MOs inactive (7;6;6;5) (hereafter π-CASSCF). The canonical π-valence MOs computed at the ground-state optimized geometry are depicted in Figure 2, where the close-lying $3b_1(D_{2d})$ MO of σ character is also included. As illustrated in many previous applications,[17−19] analysis of the nature and spacing of the canonical MOs is usually helpful and shall be employed later to rationalize the most important spectroscopic features obtained from more complex CASSCF wave functions.

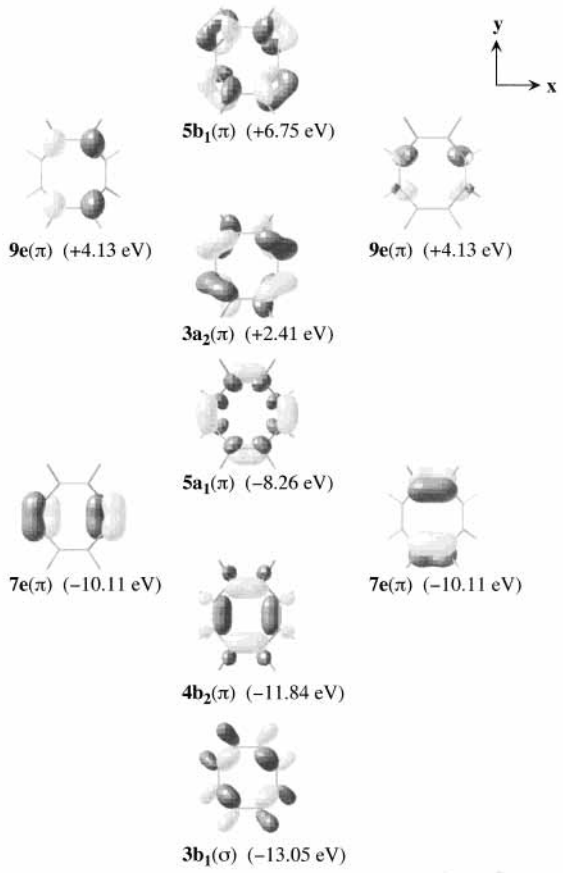

Figure 2. Highest five occupied and π-valence unoccupied canonical MOs computed with the ANO-type C,N,O[4s3p1d]/H[2s1p] basis set at the ground-state π-CASSCF equilibrium geometry of cycloocta-1,3,5,7-tetraene (see text). Orbital energies (within parentheses) are also included.

The $3b_1$, $4b_2$, 7e, $5a_1$, $3a_2$, 9e, and $5b_1$ canonical MOs (D_{2d}) are computed in C_{2v} symmetry as the $5a_2$, $8a_1$, $7b_1(7b_2)$, $9a_1$, $6a_2$, $9b_1(9b_2)$, and $9a_2$ MOs, respectively. The equilibrium geometry for the ground-state COTRA (1^2B_{1u} of the D_{4h} point group) and the lowest triplet state (1^3A_{2g} of the D_{8h} symmetry) were also determined at the same level of calculation (π-CASSCF wave function employing the valence basis set C[4s3p1d]/H[2s1p]). Using the mapping $D_{2d}/D_{4h}/D_{8h}$, the π-valence MOs in increasing ordering of orbital energy transform as follows: $b_2/a_{2u}/a_{2u}$, $e/e_g/e_{1g}$, $a_1 + a_2/b_{2u} + b_{1u}/e_{2u}$, $e/e_g/e_{3g}$, and $b_1/a_{1u}/b_{1u}$. Actual calculations of planar COT (D_{4h} and D_{8h} point groups) were carried out in C_1 symmetry. To calculate energy differences (vertical and nonvertical excitation energies, IPs, and EA), as well as for the computation of transition properties, the basis set was supplemented with two s-, two p-, and two d-type diffuse functions (see exponents elsewhere[28]) placed at the origin of the molecule. The extended basis set consists of 202 basis functions (666 primitives). The total SCF energy for ground-state COT, employing the C[4s3p1d]/H[2s1p] + 2s2p2d basis set, was calculated to be −307.619 000 au at the D_{2d} optimized geometry (see below).

The molecular orbitals of the excited states have been obtained from state average CASSCF calculations, where the averaging included the states of interest for a given symmetry.

TABLE 1: CASSCF Wave Functions Employed To Compute the Vertical Electronic Excited States of COT at the Ground-State Optimized Geometry (D_{2d} Symmetry)[a]

wave function[b]	N_e[c]	states[d]	$N_{configurations}$[e]	N_{states}[f]
		Computed States in $^1A_1(C_{2v})$ Symmetry (Inactive: 5;4;4;2)		
CASSCF(6;2;2;3)	10	$5a_1 \rightarrow 3s$, $3p_z$; $3d_{x^2-y^2}$, $3d_{z^2}$; $\pi\pi^*$; $\pi\pi^*$; $\pi\pi^*$; $4b_2 \rightarrow 3s$, $3p_z$; $3d_{x^2-y^2}$, $3d_{z^2}$; $3b_1 \rightarrow 3a_2$; $\pi\pi^*$	108 001	14
		Computed States in $^1B_1(C_{2v})$ Symmetry (Inactive: 5;4;4;3)		
CASSCF(3;4;2;3)	8	$5a_1 \rightarrow 3p_{x,y}$, $3d_{xz,yz}$; $\pi\pi^*$; $7e \rightarrow 3s$, $3d_{xy}$; $4b_2 \rightarrow 3p_{x,y}$; $\pi\pi^*$; $4b_2 \rightarrow 3d_{xz,yz}$	17 640	9
		Computed States in $^1A_2(C_{2v})$ Symmetry (Inactive: 5;4;4;3)		
CASSCF(2;2;2;3)	8	$5a_1 \rightarrow 3a_2$; $5a_1 \rightarrow 3d_{xy}$; $4b_2 \rightarrow 3a_2$; $4b_2 \rightarrow 3d_{xy}$	1 308	4

[a] Actual calculations were carried out in C_{2v} symmetry. [b] The ANO-type basis set C[4s3p1d]/H[2s1p] + 2s2p2d Rydberg functions placed at the origin were used (see text). Within parentheses are the number of orbitals of the symmetries a_1, b_1, b_2, and a_2, respectively, of the point group C_{2v}. Number of frozen orbitals: (2;2;2;2). Number of occupied SCF MOs: (9;7;7;5). The $3b_1$, $4b_2$, 7e, $5a_1$, and $3a_2$ MOs of D_{2d} symmetry correspond to the $5a_2$, $8a_1$, $7b_1(7b_2)$, $9a_1$, and $6a_2$ MOs of the C_{2v} symmetry, respectively. The character and ordering of the states are those obtained with the CASSCF method. [c] Number of active electrons. [d] Nature of the computed states according to the D_{2d} point group (see Figure 2). [e] Number of configurations in the CASSCF wave function. [f] States included in the average CASSCF wave function.

The respective CASSCF wave functions were subsequently used as reference function in a second-order perturbation treatment by means of the CASPT2 method.[15,16] In addition, the effect of weakly interacting intruder states was minimized by using the so-called imaginary level-shift technique.[29] After a careful analysis on the influence of the shift value on the spectroscopic results, the shift of 0.2 au was selected to collect the results compiled in the next section. A detailed account of the active spaces employed to compute the valence and Rydberg excited states can be found in Table 1.

In summary, the π-valence active space was extended to include the Rydberg orbitals of the different symmetries, as appropriate. Initially, we wanted to study the singlet $\rightarrow$ singlet electronic spectra up to 7 eV, since within this energy the most important features of the spectrum can be expected. Nevertheless, because of the large differential correlation energy between some valence excited states with respect to the ground state, the number of CASSCF roots had to be increased considerably. For instance, the valence state $^1B_2(3b_1 \rightarrow 3a_2)$ (D_{2d} labeling) corresponds to the thirteen root of the first set of calculations ($^1A_1(C_{2v})$) listed in Table 1. As we shall see next, this state is placed at 10.09 eV at the CASSCF level but at 6.14 eV once dynamic correlation contributions are taken into account within the framework of the CASPT2 method. As a byproduct of the required computation to consider all the excited states below 7 eV, a number of additional valence and Rydberg excited states were obtained. In the second set of calculations described in Table 1, the E($\pi\pi^*$) state responsible of the most intense transition appears as the seventh root of the CASSCF computation, above Rydberg states converging to the second and third IPs. To avoid their influence as intruder states in the treatment of the valence ^1E states, those Rydberg states had to be explicitly considered. Therefore, the π-valence active space was consequently enlarged to include the 3s and $3d_{xy}$ MOs belonging to the a_1 and a_2 irreducible representations of the C_{2v} point group. The vertical energy of each excited stated was referred to the ground-state energy computed with the same active space. Since vertical singlet $\rightarrow$ singlet and singlet $\rightarrow$ triplet electronic spectra were computed in C_{2v} symmetry and dynamic correlation effects have a tremendous influence to determine accurately several important transitions, the computation turned out to be particularly challenging from a technical standpoint.

The CASSCF state interaction (CASSI) method[30,31] was used to calculate the transition dipole moments. In the formula for the oscillator strength the CASSCF transition moment and the energy difference obtained in the CASPT2 computation were used.

All calculations were performed with the MOLCAS-5 quantum chemistry software.[32]

TABLE 2: Computed CASSCF and CASPT2 Excitation Energies (eV) and Related Oscillator Strengths (*f*) for the Vertical Singlet−Singlet Electronic Transitions of COT (D_{2d} Symmetry) Employing the C,N,O[4s3p1d]/H[2s1p] + 2s2p2d (Rydberg Functions) ANO-Type Basis Set[a]

state[b]	CASSCF	CASPT2	*f*	experimental
		Singlet Excited States up to 7 eV		
$1^1A_2(5a_1 \rightarrow 3a_2)$	6.70	3.79	forbidden	4.39,[c] 4.43,[d] 4.39[e]
$1^1E(\pi\pi^*)$	7.88	5.56	0.0075	
$2^1A_1(5a_1 \rightarrow 3s)$	5.81	5.58	forbidden	
$2^1E(5a_1 \rightarrow 3p_{x,y})$	6.69	5.93	0.0004	
$3^1A_1(\pi\pi^*)$	6.84	6.14	forbidden	
$1^1B_2(3b_1 \rightarrow 3a_2)$	10.09	6.14	0.0111	
$2^1B_2(5a_1 \rightarrow 3p_z)$	6.21	6.17	0.0532	6.05,[c] 6.02[d]
$1^1B_1(4b_2 \rightarrow 3a_2)$	8.02	6.36	forbidden	
$3^1E(\pi\pi^*)$	10.28	6.40	1.1096	6.42,[c,d] 6.16[e]
$4^1A_1(5a_1 \rightarrow 3d_{z^2})$	6.76	6.57	forbidden	
$3^1B_2(5a_1 \rightarrow 3d_{xy})$	7.22	6.71	(−)[f]	
$4^1E(5a_1 \rightarrow 3d_{xz,yz})$	7.35	6.78	0.0014	
$2^1B_1(5a_1 \rightarrow 3d_{x^2-y^2})$	6.75	6.80	forbidden	
		Additional Valence States		
$^1A_1(\pi\pi^*)$	8.72	7.41	forbidden	
$^1B_2(\pi\pi^*)$	8.38	7.68	0.0001	
$^1A_1(\pi\pi^*)$	10.57	7.98	forbidden	
		Additional Rydberg States		
$^1E(7e \rightarrow 3s)$	8.12	7.04	0.0409	6.99[d]
$^1E(7e \rightarrow 3d_{xy})$	8.86	8.24	0.0002	
$^1B_2(4b_2 \rightarrow 3s)$	8.93	8.39	0.0250	8.41[d]
$^1E(4b_2 \rightarrow 3p_{x,y})$	9.90	8.80	0.0390	
$^1A_1(4b_2 \rightarrow 3p_z)$	9.32	8.95	forbidden	
$^1E(4b_2 \rightarrow 3d_{xz,yz})$	10.50	9.26	0.1346	9.05[d]
$^1A_1(4b_2 \rightarrow 3d_{xy})$	10.35	9.49	forbidden	
$^1A_2(4b_2 \rightarrow 3d_{x^2-y^2})$	9.86	9.58	forbidden	
$^1B_2(4b_2 \rightarrow 3d_{z^2})$	9.88	9.62	0.0187	

[a] Experimental data are also included. [b] The character and ordering of the states are those obtained with the CASPT2 method. [c] From the optical spectrum.[5,8] [d] EELS data.[3] [e] From the absorption spectrum in hexane.[4] [f] The state was computed in A_2 (C_{2v}) symmetry, and *f* could not be computed because the transition is dipole forbidden.

3. Results and Discussion

3.1. Vertical Singlet $\rightarrow$ Singlet Electronic Transitions. The vertical singlet $\rightarrow$ singlet electronic transitions were computed at the π-CASSCF equilibrium geometry of COT. The optimized parameters, r(C═C) = 1.341 Å, r(C−C) = 1.477 Å, r(C−H) = 1.078 Å, ∠(C═C−C) = 127.1°, ∠(C═C−H) = 117.6°, ∠(C═C−C═C) = 55.1°, are close to those reported in the ED study (r(C═C) = 1.340 Å, r(C−C) = 1.476 Å, ∠(C═C−C) = 126.1°, ∠(C═C−H) = 117.6°).[9] The results obtained by means of the CASSCF/CASPT2 procedure are collected in Table 2. The first column identifies the excited states of the COT molecule (labeling according to the D_{2d} point group). The second and third columns report the vertical excitation energy computed at the CASSCF and CASPT2 levels, respectively. The difference between those two energies is a measure of the contribution of the differential dynamic correlation effects to the vertical

excitation energy of the state. The computed oscillator strength is listed in the fourth column. Finally, the available experimental data are compiled on the right-hand side of Table 2.

The lowest singlet excited state of COT has A_2 symmetry. In terms of the corresponding natural orbitals (NOs), the CASSCF wave function is dominated by a singly excited configuration. The NOs involved are homologous to the highest occupied MO (HOMO) and the lowest unoccupied MO (LUMO): the one-electron promotion $5a_1 \rightarrow 3a_2$ (cf. Figure 2). That the lowest singlet $\rightarrow$ singlet transition is electric-dipole forbidden was clearly established by Frueholz and Kuppermann[3] in 1978. The computed vertical excitation energy at about 3.8 eV (CASPT2 result) is somewhat too low compared to the maximum of the low-intensity band observed in the optical[5,8] (4.39 eV) and EELS[3] (4.43 eV) studies. However, the previous ab initio MRCI result reported by Palmer[7] predicted the lowest-energy band to peak at 4.37 eV. The origin of the discrepancy between the MRCI result and the present finding can be attributed to the limited basis set (split-valence quality) employed for the MRCI calculations.[7] In fact, employing the current ANO-type basis set with the contraction C[3s2p]/H[2s], the CASPT2 method yields 4.45 eV, consistent with the earlier MRCI result. Adding polarization functions on the carbon atoms, C[3s2p1d]/H[2s] basis set, the excitation energy drops to 3.92 eV, consistent with our previous CASPT2/6-31G* result (4.00 eV).[1] With the largest contraction tested from the same primitive sets,[26] C[5s4p2d1f]/H[3s2p1d], the vertical transition is computed to be 3.80 eV, nearly the same as that compiled in Table 2. Therefore, 3.8−4.0 eV is so far the best theoretical estimate for the lowest vertical feature of COT. This implies that the observed band maximum and the computed vertical transition have an energy difference of about half an electronvolt. Possible sources of such a deviation have been discussed elsewhere.[1]

As can be inferred from Table 2, states denoted by $\pi\pi^*$, with no explicit mention of the configurations involved, have CASSCF wave functions with a character remarkably multiconfigurational. That is, two or more configurations have large weights in the corresponding CASSCF wave function. On the contrary, when the CASSCF wave function has only one configuration with a pronounced weight (larger than 70%), an explicit assignment is given. In particular, the $1^1E(\pi\pi^*)$ and $3^1E(\pi\pi^*)$ states are described mainly by a linear combination of two singly excited configurations related to the HOMO − 1 → LUMO and HOMO → LUMO + 1 one-electron promotions. According to the orbital energies given in Figure 2, the energy difference between the orbital energies of LUMO/HOMO − 1 and LUMO + 1/HOMO is 12.52 and 12.39 eV. Therefore, those two one-electron promotions are nearly degenerate and can further interact, leading to minus and plus linear combinations, which rationalizes the CASSCF findings. Energetically, as a result of the interaction, the minus and plus states are pushed down and up, respectively. The electronic transition related to the former is predicted with low intensity (the respective transition moments are subtracted), and the latter should carry most of the intensity. This is indeed the case. The $1^1E(\pi\pi^*)$ and $3^1E(\pi\pi^*)$ states are computed vertically at 5.56 and 6.40 eV, respectively. The transition from the ground to the $3^1E(\pi\pi^*)$ state is predicted to be the most intense feature of the spectrum, with a calculated oscillator strength of about 1.1. The oscillator strength for the transition $1^1A_1 \rightarrow 1^1E(\pi\pi^*)$ is, however, relatively small (0.008). The weights of the (HOMO → LUMO + 1, HOMO − 1 → LUMO) one-electron promotions in the respective CASSCF wave function are (in percentage) (15, 29) (1^1E) and (22, 40) (3^1E). The apparent good agreement between the computed excitation energy for the transition $1^1A_1 \rightarrow 3^1E(\pi\pi^*)$ (6.40 eV) with respect to the observed maximum (6.42 eV)[3,5,8] is somewhat fortuitous. The computed vertical excitation energy for the $3^1E(\pi\pi^*)$ state is estimated to have an accuracy of ±0.2 eV, somewhat larger than the usual error bars of the method in similar applications (molecules of relatively small molecular size with extended ANO-type basis sets).[17−19] As stated above, the $3^1E(\pi\pi^*)$ state has large dynamic correlation contributions, appearing as a high root in the average CASSCF procedure, and many weakly interacting states behave as intruders. Most of them are removed with the employed active space beyond the π-valence active space, together with the imaginary level shift technique, but still some influence remains. The excitation energies for Rydberg states described in the same calculation as the valence ^1E states (see Table 1) are, however, stable and expected to have the usual accuracy of the method (±0.1 eV). Despite these technical problems, the most intense feature of the spectrum can be unambiguously assigned to the electronic transition $1^1A_1 \rightarrow 3^1E(\pi\pi^*)$, confirming the pioneering theoretical assignment performed by Van-Catledge in 1971 on the basis of INDO results.[6] Apart from our preliminary results reported recently,[1] only this INDO study[6] characterizes the computed electronic transitions by both excitation energies and oscillator strengths. It is clear that both properties are equally relevant to perform spectroscopic assignments.

TABLE 3: Computed CASSCF and CASPT2 Vertical Ionization Potentials (IPs) for COT Employing the C,N,O[4s3p1d]/H[2s1p] + 2s2p2d (Rydberg Functions) ANO-Type Basis Set

IP[a]	state	CASSCF	CASPT2	experimental[b]
IP_1	$1^2A_1(\pi\text{-hole})$	8.26	8.08	8.42
IP_2	$1^2E(\pi\text{-hole})$	9.58	9.66	9.78
IP_3	$1^2B_2(\pi\text{-hole})$	11.32	10.80	11.15
	$1^2B_1(\sigma\text{-hole})$	12.46	10.95	
	$1^2A_2(5a_1 \rightarrow 3a_2)$	11.60	11.10	

[a] The character and ordering of the states are those obtained with the CASPT2 method. Results in eV. [b] Data taken from the PE spectrum of COT.[20]

Between the $1^1E(\pi\pi^*)$ and $3^1E(\pi\pi^*)$ states, three valence states are found. At the CASPT2 level, the $3^1A_1(\pi\pi^*)$ and $1^1B_2(3b_1 \rightarrow 3a_2)$ states are computed to be degenerated at 6.14 eV. The $1^1B_1(4b_2 \rightarrow 3a_2)$ state lies at 6.36 eV above the ground state, close to the $3^1E(\pi\pi^*)$ state. The $3^1A_1(\pi\pi^*)$ state has a doubly excited character, with a prominent weight (33.2%) of the doubly excited configuration $(\text{HOMO} \rightarrow \text{LUMO})^2$. The $1^1B_2(3b_1 \rightarrow 3a_2)$ state is described mainly by the one-electron promotion from the highest σ orbital ($3b_1$) to the LUMO. The oscillator strength for the transition $1^1A_1 \rightarrow 1^1B_2$ is 0.011, and therefore, it can contribute to some extent to the shoulder recorded in the spectrum at about 6 eV.[3,5,8] Incidentally, the transition $1^1A_1 \rightarrow 1^1E(\pi\pi^*)$ was previously related to the observed shoulder, but this is not confirmed by the present results. Instead, we propose the transition from the ground state to the Rydberg state $2^1B_2(5a_1 \rightarrow 3p_z)$ computed at 6.17 eV, with oscillator strength 0.05, as the most plausible candidate responsible for the recorded shoulder in the gas phase at 6.02 eV.[3] Our assignment of Rydberg character for the shoulder is consistent with the fact that it is not observed in the absorption spectrum of COT in hexane (band maximum at 4.39 and 6.16 eV).[4] As it is well-known Rydberg states as usually perturbed in condensed phases and collapse in solution.[33]

To design the number of Rydberg series to consider in the study, the lowest ionization potentials were calculated. The results are listed in Table 3, together with the selected experimental data taken from the PE spectrum.[20]

As previously suggested by different authors,[3,7] according to the Koopmans' theorem, the lowest four IPs, determined experimentally[20−22] at 8.42, 9.78, 11.15, and 11.55 eV, could be related to the 1^2A_1, 1^2E, 1^2B_2, and 1^2B_1 states of the COT radical cation (cf. Figure 2). From the CASPT2 results (see Table 3) one can easily conclude that the assignments based on the Koopmans' theorem are correct for the first (IP_1) and second (IP_2) ionization potentials. Three states are, however, found at about 11 eV (IP_3): $1^2B_2(\pi$-hole), $1^2B_1(\sigma$-hole), and $1^2A_2(5a_1 \rightarrow 3a_2)$. The latter is a non-Koopmans state and, therefore, is not visible in the PE spectrum. As pointed out by Palmer,[7] the most intense feature in this energy region of the PE spectrum can probably be related to the $1^2B_2(\pi$-hole) state. Nevertheless, the results rule out the Koopmans-based assignment for the fourth IP (IP_4) because the 1^2B_1 state is placed around 11 eV, that is, 0.7 eV below the observed IP_4 at 11.55 eV. Therefore, IP_4 cannot be assigned from the current results. The computed gaps between the second-first (1.58 eV) and third-second PE bands (1.14 eV) are consistent with previous theoretical predictions at the CASPT2/6-31G* level, 1.42 and 1.08 eV, respectively.[34] In the recorded PE spectrum[20] of COT, the spacing between the first three bands is, however, equal (1.37 eV). Deviations between the theoretical and experimental vertical ionization potentials (especially for IP_1 and IP_3) seem to point out that the observed peaks might not correspond to the vertical ejection of the electron or/and the cation does not retain the COT structure (see discussion in ref 34).

The first and second vertical ionization potentials of COT lie within 1.58 eV of each other (CASPT2 results). As a consequence, corresponding members of the Rydberg series converging to these two ionization potentials are expected to lie within 1.5−1.6 eV of each other. Consistently, the energy difference between the $^1E(7e \rightarrow 3s)$ and $2^1A_1(5a_1 \rightarrow 3s)$ states is computed to be 1.46 eV. The $^1B_2(4b_2 \rightarrow 3s)$ state appears at 8.39 eV, that is, 1.35 eV above the $^1E(7e \rightarrow 3s)$ state. That energy difference can be related to the energy difference IP_3-IP_2 (1.14 eV). As 1−1.5 eV approximates the usual 3s and 3d Rydberg-state separation, the early series members leading to the first ionization limit are not expected to overlap in energy with the remaining members. Therefore, the main target of the study was to characterize the 3s, 3p, and 3d members of the Rydberg series converging to the first IP. As stated in the previous section, to gather the valence states below 7 eV, a number of additional Rydberg states were also obtained because of the intrinsic difficulties of the COT system and available software.[32] (MOLCAS-5 does not offer the possibility to treat the COT system within D_{2d} symmetry, and actual calculations were performed within the C_{2v} point group).

The lowest Rydberg state, the $2^1A_1(5a_1 \rightarrow 3s)$ state, is predicted at 5.58 eV. Frueholz and Kuppermann[3] saw no evidence of the $5a_1 \rightarrow 3s$ member in their electron impact spectra. They remarked, however, that the 3s feature should be near 5.2 eV.[3] Transition to the $2^1E(5a_1 \rightarrow 3p_{x,y})$ state is computed somewhat above, at 5.93 eV, with an exceedingly small oscillator strength. The $2^1B_2(5a_1 \rightarrow 3p_z)$ state can be clearly related to the observed shoulder at 6.02 eV.[3] The $5a_1 \rightarrow 3d$ members are computed within the energy range 6.57−6.80 eV (average value 6.73 eV).

The average of the excitation energies corresponding to the $5a_1 \rightarrow 3p$ is 6.01 eV. Adding to it the energy difference IP_2-IP_1 (1.58 eV) gives 7.59 eV, as an estimate for the $7e \rightarrow 3p$ average excitation energies, which were not directly computed. Adding 1.14 eV (IP_3-IP_2) to 7.59 eV is equal to 8.73 eV, the expected average excitation energies of the members $4b_2 \rightarrow 3p$, which is consistent with the average value obtained for the corresponding CASPT2 results (8.85 eV) (cf. Table 2). Employing a similar reasoning, the $7e \rightarrow 3d$ members are predicted around 8.2−8.3 eV.

TABLE 4: Computed CASSCF and CASPT2 Excitation Energies (eV) for the Low-Lying Triplet Excited States of COT Employing the C,N,O[4s3p1d]/H[2s1p] + 2s2p2d (Rydberg Functions) ANO-Type Basis Set[a]

state	transition	CASSCF	CASPT2	experimental
$1^3A_2(5a_1 \rightarrow 3a_2)$	S−T vertical	3.66	2.82	3.05,[b] 2.89[c]
	S−T 0−0	1.42	0.78	
	emission max.	0.66	0.22	
$1^3E(\pi\pi^*)$	S−T vertical	4.31	3.84	4.05[b]
$1^3B_1(\pi\pi^*)$	S−T vertical	5.18	4.69	4.84[b]
$1^3A_1(5a_1 \rightarrow 3s)$	S−T vertical	6.04	5.54	

[a] Experimental data are also included. [b] EELS data.[3] [c] From a kinetic analysis[14] employing the experimental donor triplet energies reported elsewhere.[12,13]

Despite the fact that we have a number of missing states in the computed spectrum between 7 and 8 eV, the additional transitions observed by EELS[3] at 6.99, 8.41, and 9.05 eV may be tentatively assigned. The former can be related to the $1^1A_1 \rightarrow {}^1E(7e \rightarrow 3s)$ transition, computed at 7.04 eV with oscillator strength 0.04. The two fairly intense transitions observed at 8.41 and 9.05 eV are consistent with the results for the vertical transition from the ground to the $^1B_2(4b_2 \rightarrow 3s)$ and $^1E(4b_2 \rightarrow 3d_{xz,yz})$ states with the excitation energies (oscillator strengths) 8.39 eV (0.03) and 9.26 eV (0.13), respectively.

3.2. Low-Lying Triplet States. The CASSCF and CASPT2 results computed for the low-lying triplet states are compiled in Table 4. Three valence singlet → triplet vertical transitions are found below the $1^3A_1(5a_1 \rightarrow 3s)$ state, the lowest excited state of Rydberg character, placed at 5.54 eV. Those valence features lie at 2.82, 3.84, and 4.69 eV above the ground state and can be related to the three transitions reported by Frueholz and Kuppermann[3] at 3.05, 4.05, and 4.84 eV, which were identified by these authors as singlet → triplet transitions. Therefore, according to the current computation, those observed singlet → triplet transitions can be assigned as the $1^1A_1 \rightarrow 1^3A_2(5a_1 \rightarrow 3a_2)$, $1^1A_1 \rightarrow 1^3E(\pi\pi^*)$, and $1^1A_1 \rightarrow 1^3B_1(\pi\pi^*)$ transitions. Our assignments for the two lowest transitions confirm those performed by Palmer[7] on the basis of limited CI calculations and small basis sets, although the $1^3E(\pi\pi^*)$ state was placed higher by more than 1 eV. The CASPT2 results suggest, however, that the $1^3B_1(\pi\pi^*)$ state is responsible for the third observed band. In the CI calculations of Palmer the 2^3A_2 state is found as the third-energy triplet state, although a $^1B_1$ state was also found to be energetically close. The CASPT2 calculation places the 2^3A_2 state (not shown in Table 4) about 2.5 eV above the 1^3B_1 state, that is about 0.7 eV above the lowest Rydberg triplet state.

A systematic deviation of the CASPT2 vertical singlet → triplet transitions with respect to the EELS data is noted (cf. Table 4). The CASPT2 method seems to underestimate those by about 0.2 eV. It can be partially related to the employed zeroth-order Hamiltonian (Møller−Plesset type) that favors open-shell systems and leads to triplet states somewhat too low. It is a well-documented effect, and an interested reader can obtain further information about it elsewhere (see, for instance, ref 18, where a pedagogic status of the issue is developed, as well as the original references therein). Since here there is no controversy in the assignments, additional checks employing more sophisticated zeroth-order Hamiltonians were not performed. Moreover, from the available triplet−triplet energy transfer experiments contradictory results were suggested for

the vertical singlet−triplet excitation energy.[12,13] However, applying our recently proposed theoretical model[14] to the same experimental data,[12,13] we predict that the vertical singlet−triplet transition energy is 2.89 eV, close to the computed value of 2.82 eV.

To a good approximation, the $1^3A_2(5a_1 \rightarrow 3a_2)$ state can be described by the one-electron promotion HOMO → LUMO. The π-CASSCF wave function of the $1^3E(\pi\pi^*)$ state is composed of a linear combination of two singly excited configurations: HOMO − 1 → LUMO (49.6%) and HOMO → LUMO + 1 (37.4%). The $1^3B_1(\pi\pi^*)$ state really has a multiconfigurational character with weights spread over many different configurations equally important.

The 0−0 excitation energy and the phosphorescence maximum were also computed for the lowest singlet → triplet transition. We were motivated by the possible significance of the lowest-lying triplet state of COT in the triplet quenching process of laser dye solutions (for instance, rhodamine bG). The equilibrium geometry of the lowest triplet excited state is octogonal (D_{8h} symmetry).[35] The π-CASSCF optimized parameters, employing the ANO-type C[4s3p1d]/H[2s1p] basis set, are r(C−C) = 1.404 Å and r(C−H) = 1.077 Å. The adiabatic excitation or 0−0 band origin is computed as the energy difference between the triplet state ($1^3A_{2g}(D_{8h})$) and the ground state ($1^1A_1(D_{2d})$) at their respective equilibrium geometries. No zero point energy (ZPE) corrections were included. In this manner, the 0−0 excitation energy is computed to be 0.78 eV at the CASPT2 level. ZPE could contribute at most 0.1 eV, which is within the intrinsic error bars of the CASPT2 method. Within this level of approximation, the energy difference between the vertical and adiabatic excitation energy accounts for the geometry relaxation of the triplet excited state. Therefore, simultaneously to the electronic excitation of COT, a progressive structural reorganization toward planarity takes place. Because the energy difference between the vertical and 0−0 excitation energies of the $S_0 \rightarrow T_1$ transition is large, about 2 eV, COT has a pronounced nonvertical behavior and covers a wide range of triplet donors.[12−14] Moreover, the origin of the $S_0 \rightarrow T_1$ transition, about 0.8 eV, can be considered as an estimate of the lower limit for the triplet energy of a donor that the acceptor COT could still react with.

The phosphorescence maximum is predicted by computing the ground ($1^1B_{2g}(D_{8h})$) and triplet ($1^3A_{2g}(D_{8h})$) states at the equilibrium geometry of the triplet state. The computed phosphorescence maximum, 0.22 eV, lies in the infrared range. The current estimate is consistent with previous ab initio results for the singlet−triplet splitting of D_{8h} COT reported by Hrovat and Borden.[35] They found that the triplet state has a higher ZPE than the singlet by 2.1 kcal/mol at the planar geometry. That the ground state at the D_{8h} symmetry is a singlet state (1^1B_{2g}) and therefore the molecule violates the Hund's rule is by now well established (see the elegant 1996 paper by Wenthold et al.,[23] which is a landmark contribution on this issue). An alternative and interesting view is, of course, that in antiaromatic molecules the Hund's rule is not expected to hold, as was clearly suggested two years later by Zilberg and Haas.[36]

Additional information about the lowest triplet state was obtained from the PE spectrum of planar COTRA,[23,24] where photodetachment to two distinct electronic states of neutral COT was observed. Wenthold *et al.*[23] identified these electronic states as the $1^1A_{1g}(D_{4h})$ state, corresponding to the transition state of COT ring inversion along the S_0 hypersurface, and the $1^3A_{2g}(D_{8h})$ state, recorded at 1.10 and 1.62 eV, respectively. Incidentally, the ground-state potential energy hypersurface of COT has been, and still is, a subject of great theoretical attention.[1,23,37−40] It is known that the ground state of neutral COT has four equivalent D_{2d} local minima connected by two independent reaction paths: ring inversion (D_{4h} transition state) and bond shifting (D_{8h} transition state). The vertical PE spectrum of planar COTRA and the EA of COT obtained at the π-CASSCF and CASPT2 levels of theory are compiled, together with available experimental data, in Table 5.

TABLE 5: Computed PE Spectrum of the Planar Cyclooctatetraene Radical Anion (COTRA) and the Electron Affinity (EA) of COT Employing the C,N,O[4s3p1d]/H[2s1p] + 2s2p2d (Rydberg Functions) ANO-Type Basis Set[a]

state	CASSCF	CASPT2	experimental
Ground State of COTRA (1^2B_{1u}) (D_{4h} Symmetry)			
1^1A_{1g}	−0.86	1.11	1.10[b]
1^3A_{2g}	0.16	1.47	1.62[b]
vertical EA	−2.79	−0.46	
adiabatic EA	−1.43	0.56	0.58[c]

[a] Energy differences in eV. Experimental data are also included. [b] Taken from the PE spectrum of COTRA.[23] [c] Determined by the kinetic method. See ref 25 and also references therein.

The ground-state (1^2B_{1u}) equilibrium geometry of the COTRA system belongs to the D_{4h} point group. Its π-CASSCF optimized parameters are r(C═C) = 1.375 Å, r(C−C) = 1.437 Å, r(C−H) = 1.081 Å, and ∠(C═C−C) 135.0°. Employing this structure, the ground state of the neutral system is computed to be vertically at 1.11 eV and the lowest triplet state to be at 1.47 eV, in agreement with the experimental data.[23] As detailed in Table 5, those are results obtained at the CASPT2 level. The nondynamical correlation effects treated by the CASSCF method are certainly not enough to predict accurately (within 0.2 eV) the energy differences between the ground state of COTRA and the considered states of the neutral system. It is amazing that the tremendous differential dynamical correlation between the two states can be handled just at a second-order level in a balanced way. In this type of difficult case, involving large differential dynamic correlation effects, the CASPT2 method certainly plays an outstanding role. In other words, a minus sign in the CASSCF energy difference means that COTRA is not bound at that level of theory and the CASPT2 approach is capable of recovering (qualitatively and quantitatively) the right relative position between the respective states of the anionic and neutral systems.

The vertical electron affinity is negative at both CASSCF and CASPT2 levels of theory. Therefore, we can confidently conclude that COTRA is not bound at the ground-state equilibrium geometry of COT, $1^1A_1(D_{2d})$. In addition, the computed CASPT2 adiabatic electron affinity, 0.56 eV, is in agreement with the most recent experimental determinations.[25] The agreement is entirely due to the inclusion of dynamic correlation because the ground-state radical anion is above the ground state of the neutral system by >1 eV at the π-CASSCF level (−1.43 eV in Table 5). A question arises here: Does the geometry optimization of ground-state COTRA at the CASSCF level make any sense? Previous experience dealing with true temporary anion states (for instance, in biphenyl[41] and *p*-semibenzoquinone[42] radical anions) gives a clue to answer this question. Yes, the CASSCF wave function represents in such a case a localized solution, which can be regarded as a discrete representation of the temporary anion states (see the discussion in ref 41 and the different resonance types in ref 42).

Assuming that the geometry of ground-state COTRA is similar to the D_{4h} structure of the neutral system corresponding to the transition state of COT for the ring inversion path, the barrier height of that process can be easily estimated. From the

computed PE spectrum one can obtain directly that the origin of the triplet is 0.36 eV above the lowest energy planar D_{4h} singlet state. Combining this value with the computed 0−0 excitation energy for the lowest singlet → triplet transition (0.78 eV), we estimate that the transition state for ring inversion of COT lies about 0.42 eV above the ground state, consistent with previous experimental and theoretical determinations.[1,23]

4. Summary and Conclusions

The excited states of COT were studied using ab initio quantum-chemical methods based on multiconfigurational wave functions. Employing the optimized geometry of the ground state at the CASSCF level, the vertical excitation energies were computed with the CASPT2 method. The calculation comprised both valence and Rydberg excited states in the singlet manifold. In particular, the 3s, 3p, and 3d members of the Rydberg series converging to the first ionization potential were explicitly taken into account. As a byproduct of the required computation to include all the excited states up to 7 eV, additional valence and Rydberg states were also characterized. The computed excited states 1^1A_2 (3.79 eV), $2^1B_2(3p_z)$ (6.17 eV), and 3^1E (6.40 eV) are related to the main singlet → singlet features observed experimentally, that is, the low-energy, low-intensity band (maximum at 4.43 eV), a shoulder at 6.02 eV, and an intense band with a maximum at 6.42 eV, respectively. On the other hand, the observed spin-forbidden singlet → triplet bands with maxima at 3.05, 4.05, and 4.84 eV are assigned as the transitions $1^1A_1 \rightarrow 1^3A_2$, $1^1A_1 \rightarrow 1^3E$, and $1^1A_1 \rightarrow 1^3B_1$, respectively. The lowest (3s) Rydberg singlet and triplet states are placed at 5.58 (2^1A_1) and 5.54 (1^3A_1) eV. In addition, new assignments are tentatively suggested for the recorded higher-energy peaks in the singlet manifold at 6.99, 8.41, and 9.05 eV. The three lowest ionization potentials are also characterized. The computed adiabatic electron affinity is 0.56 eV, in agreement with experimental determinations. Nevertheless, the COT radical anion is not bound at the equilibrium geometry of the neutral molecule.

As regards the role of COT as an efficient triplet quencher of laser dye solutions, the computation supports the nonvertical process of triplet energy transfer. Within a nonvertical energy-transfer scheme, it is predicted that COT could act as acceptor with donors having a triplet excited-state energy equal to or higher than 0.78 eV, which corresponds to the computed $S_0 \rightarrow T_1$ adiabatic excitation energy of the system. The experimental confirmation of this prediction would certainly be of great value.

Acknowledgment. Financial support through Projects BQU2000/0646, BQU2001-2926, and BQU2001-5037-ES from the Spanish Ministerio de Educación, Cultura y Deporte (MECD) and by the Generalitat Valenciana is gratefully acknowledged. L.M.F. thanks the MECD for a Doctoral Fellowship.

References and Notes

(1) Garavelli, M.; Bernardi, F.; Cembran, A.; Castaño, O.; Frutos, L. M.; Merchán, M.; Olivucci, M. *J. Am. Chem. Soc.* **2002**, *124*, 13770 and references therein.

(2) Langseth, A.; Brodersen, S. *Acta Chem. Scand.* **1949**, *3*, 778.

(3) Frueholz, R. P.; Kuppermann, A. *J. Chem. Phys.* **1978**, *69*, 3614.

(4) Perkampus, H.-H. In *UV−Vis Atlas of Organic Compounds*; Perkampus, H.-H., Ed.; VCH: Weinheim, 1992; p 135.

(5) Allinger, N. L.; Miller, M. A.; Chow, L. W.; Ford, R. A.; Graham, J. C. *J. Am. Chem. Soc.* **1965**, *87*, 3430.

(6) Van-Catledge, F. A. *J. Am. Chem. Soc.* **1971**, *93*, 4365.

(7) Palmer, M. H. *J. Mol. Struct.* **1988**, *178*, 79.

(8) Hassenrück, K.; Martin, H.-D.; Walsh, R. *Chem. Rev.* **1989**, *89*, 1125 and references therein.

(9) Traetteberg, M. *Acta Chem. Scand.* **1966**, *20*, 1724.

(10) Roos, B. O.; Merchán, M.; McDiarmid, R.; Xing, X. *J. Am. Chem. Soc.* **1994**, *116*, 5927.

(11) Serrano-Andrés, L.; Lindh, R.; Roos, B. O.; Merchán, M. *J. Phys. Chem.* **1993**, *97*, 9360.

(12) Forward, P. J.; Gorman, A. A.; Hamblett, I. *J. Chem. Soc., Chem. Commun.* **1993**, 250.

(13) Das, T. N.; Priyadarsini, K. I. *J. Chem. Soc., Faraday Trans.* **1994**, *90*, 963.

(14) Frutos, L. M.; Castaño, O.; Andrés, J. L.; Merchán, M.; Acuña, A. U. Triplet energy transfer to cycloocta-1,3,5,7-tetraene: A theoretical description of the anti-Arrhenius *nonvertical* process in terms of accurate potential energy surfaces. Submitted for publication.

(15) Andersson, K.; Malmqvist, P.-Å.; Roos, B. O.; Sadlej, A. J.; Wolinski, K. *J. Phys. Chem.* **1990**, *94*, 5483.

(16) Andersson, K.; Malmqvist, P.-Å.; Roos, B. O. *J. Chem. Phys.* **1992**, *96*, 1218.

(17) Roos, B. O.; Fülscher, M. P.; Malmqvist, P.-Å.; Merchán, M.; Serrano-Andrés, L. In *Theoretical Studies of Electronic Spectra of Organic Molecules*; Langhoff, S. R., Ed.; Kluwer Academic Publishers: Dordrecht, The Netherlands, 1995; p 357.

(18) Roos, B. O.; Andersson, K.; Fülscher, M. P.; Malmqvist, P.-Å.; Serrano-Andrés, L.; Pierloot, K.; Merchán, M. In *Multiconfigurational Perturbation Theory: Applications in Electronic Spectroscopy*; Prigogine, I., Rice, S. A., Eds.; J. Wiley & Sons: New York, 1996; p 219; *Adv. Chem. Phys.* **1996**, *93*, 219.

(19) Merchán, M.; Serrano-Andrés, L.; Fülscher, M. P.; Roos, B. O. In *Multiconfigurational Perturbation Theory Applied to Excited States of Organic Compounds*; Hirao, K., Ed.; World Scientific Publishing Company: Amsterdam, 1999; Vol. 4, p 161.

(20) Batich, C.; Bischof, P.; Heilbronner, E. *J. Electron Spectrosc. Relat. Phenom.* **1972/73**, *1*, 333.

(21) Bieri, G.; Burger, F.; Heilbronner, E.; Maier, J. P. *Helv. Chim. Acta* **1977**, *60*, 2213.

(22) Kobayashi, T. *Phys. Lett.* **1979**, *A70*, 292.

(23) Wenthold, P. G.; Hrovat, D. A.; Borden, W. T.; Lineberger, W. C. *Science* **1996**, *272*, 1456.

(24) Wenthold, P. G.; Lineberger, W. C. *Acc. Chem. Res.* **1999**, *32*, 597.

(25) Denault, J. W.; Chen, G. D.; Cooks, R. G. *J. Am. Chem. Soc. Mass Spectrom.* **1998**, *9*, 1141 and references therein.

(26) Widmark, P.-O.; Malmqvist, P.-Å.; Roos, B. O. *Theor. Chim. Acta* **1990**, *77*, 291.

(27) For reviews of the CASSCF methods, see different contributions in: *Ab Initio Methods in Quantum Chem.-II*; Lawley, K. P., Ed.; J. Wiley & Sons Ltd.: New York, 1987.

(28) Rubio, M.; Merchán, M.; Ortí, E.; Roos, B. O. *Chem. Phys.* **1994**, *179*, 395.

(29) Forsberg, N.; Malmqvist, P.-Å. *Chem. Phys. Lett.* **1997**, *274*, 196.

(30) Malmqvist, P.-Å. *Int. J. Quantum Chem.* **1986**, *30*, 479.

(31) Malmqvist, P.-Å.; Roos, B. O. *Chem. Phys. Lett.* **1989**, *155*, 189.

(32) Andersson, K.; Baryz, M.; Bernhardsson, A.; Blomberg, M. R. A.; Boussard, P.; Cooper, D. L.; Fleig, T.; Fülscher, M. P.; Hess, B.; Karlström, G.; Lindh, R.; Malmqvist, P.-Å.; Neogrády, P.; Olsen, J.; Roos, B. O.; Sadlej, A. J.; Schimmelpfennig, B.; Schütz, M.; Seijo, L.; Serrano-Andrés, L.; Siegbahn, P. E. M.; Stålring, J.; Thorsteinsson, T.; Veryazov, V.; Wahlgren, U.; Widmark, P.-O. *MOLCAS, version 5.0*; Department of Theoretical Chemistry, Chemical Centre, University of Lund: P. O. B. 124, S-221 00 Lund, Sweden, 2000.

(33) Robin, M. B. *Higher Excited States of Polyatomic Molecules*; Academic Press: New York, 1975; Vols. I, II, and III.

(34) Bally, T.; Truttmann, L.; Dai, S.; Williams, F. *J. Am. Chem. Soc.* **1995**, *117*, 7916.

(35) Hrovat, D. A.; Borden, W. T. *THEOCHEM* **1997**, *398−399*, 211.

(36) Zilberg, A.; Haas, Y. *J. Phys. Chem. A* **1998**, 102, 10851.

(37) Andrés, J. L.; Castaño, O.; Morreale, A.; Palmeiro, R.; Gomperts, R. *J. Chem. Phys.* **1998**, *108*, 203.

(38) Wiberg, K. B. *Chem. Rev.* **2001**, *101*, 1317.

(39) Bearpark, M. J.; Blancafort, L.; Robb, M. A. *Mol. Phys.* **2002**, *100*, 1735.

(40) Castaño, O.; Palmeiro, R.; Frutos, L. M.; Andrés, J. L. *J. Comput. Chem.* **2002**, *23*, 732.

(41) Rubio, M.; Merchán, M.; Ortí, E.; Roos, B. O. *J. Phys. Chem.* **1995**, *99*, 14980.

(42) Pou-AméRigo, R.; Serrano-Andrés, L.; Merchán, M.; Ortí, E.; Forsberg, N. *J. Am. Chem. Soc.* **2000**, *122*, 6067.